"The Application of Digital X-Radiograph Imaging for the Determination of Bulk Density"

Andrew Kowalczk
Texas A&M University of Galveston

Mentors: Patrick Dickhudt and Dr. Friedrichs

Abstract:

The improvement of digital x-radiograph imaging technology has led to the application of this technique to determine the bulk density of marine sediments. Variations in bulk density cause differential attenuation of x-rays, allowing correlation between the grayscale pixel values recorded on the digital x-ray panel and the bulk density of the sediment. This can be used to develop a predictive relationship for bulk density. Bulk density is an important sediment property related to the compaction and erodability of sediment, especially at the sediment-water interface, where there is active erosion and deposition of sediments. Samples collected were imaged using digital x-radiography, and grain size, organic content, and bulk density analyses were conducted to determine their effects on x-ray attenuation.

Methods were developed to intercalibrate x-ray images, and grain size, organic content, and bulk density analyses were also conducted upon the imaged sediment. Calibration plots and equations were developed relating grayscale pixel values to measured bulk densities of the samples. Bulk densities were calculated using these calibrations and it was shown the calibrations for individual sites yielded more accurate bulk densities that the calibration for all sites combined. Organic content and grain size were not found to produce any obvious effect on x-ray attenuation.

Applications of this technique include mapping bulk density values of sediment x-ray images, creating bulk density profiles along a core axis, and extrapolating bulk density measurements to a greater depth than mechanically analyzed. Calibrations for sites are also accurate enough to be used for other samples collected at the same sites.

Introduction:

The refinement of digital x-radiograph imaging techniques is leading to practical applications of the technique in the field of Marine Science. The advantages to using digital x-radiography to image sediment cores include high sensitivity and resolution (Migeon 1999), the consistency of the digital image relative to the older chemical film development process, and the speed at which the x-ray image is made available for further analysis. Methods have been developed to determine bulk density using CT scans and analogue x-radiographs (Orsi 1999). The development of a rapid and accurate method to find the bulk densities of sediment cores and slabs using digital x-radiograph imaging is desirable, as there are many physical and biological processes that occur after collection of the sediment that can rapidly alter the characteristics of the sediment (Wheatcroft 2005). Fast, accurate readings of the bulk densities of sediment are also closer to *in situ* values.

As x-rays pass through sediment cores, they are attenuated to varying degrees depending upon the bulk density of the sediment, which is represented by changes in the brightness of the image (Wheatcroft 2005). Sediment with a higher bulk density (lower water content) will attenuate a greater amount of x-ray energy. This will produce higher grayscale pixel values on the panel, whereas sediment with a low bulk density (higher water content) will attenuate less x-ray, and the panel will record lower grayscale pixel values. The x-ray photons that reach the digital plate pass through the sediment without interaction.

Bulk density is the absolute density of sediment including the water content of the sediment. The main controlling factor is water content, but organic content and grain size are also factors affecting bulk density. The bulk density of sediment is important because it relates to the erodability of the sediment and how certain physical and biological processes will affect it. The top layer, consisting of the top few mm to cm of sediment, is the interface layer where erosion and deposition occur (Friedrichs 2005). This layer characteristically has a low bulk density and can potentially be identified using digital x-radiograph imaging.

Multiple Factors must be accounted for when considering the attenuation of x-rays. The attenuation of an x-ray (a collimated beam of monoenergetic photons) with an initial intensity of I_o passing through a material of thickness D will result in an x-ray with a reduced intensity of I. This process is described by the equation $I = I_o\exp(-\mu D)$, known as Beer's Law. The linear attenuation coefficient, μ, is dependant primarily upon the energy of the radiation, the electron density, and the packing density of the material (Aylmore 1993). The chemical composition must be taken into account when determining the attenuation of x-rays. The size of the individual elements as well as the electron density has an effect on the linear attenuation coefficient (μ). As a result of their differing chemical compositions, organic content and the grain size fractions should theoretically have an effect upon the attenuation of x-rays.

Methods:

A Smith-Mac Grab was used to collect cores in the field at four locations in the York River, shown in Figure 1. Grabs were taken in the Clay Banks Secondary Channel, the Clay Banks Main Channel, at the VIMS buoy site, and at the Goodwin Islands at the mouth of the York to try and obtain a range of sediment types and energy regimes. Two replicate grabs were collected at each site to determine accuracy of sampling and for comparison between grain size analysis and bulk density measurements. At the first three sites, slabs for x-ray analysis and sub cores were collected from a Smith-Mac bottom sampler and sectioned off into one-centimeter intervals to a depth of ten centimeters. Grain size, organic content, and bulk density analyses were conducted upon these sediment samples. At the fourth site, sediment samples were collected by sectioning x-ray slabs at one-centimeter intervals after x-ray imaging was complete. Laboratory sediment analyses were then performed on these samples to determine grain size distribution, bulk density, and organic content.

The sub-samples were used to determine grain size and bulk density for each centimeter interval from each grab. Grain size analysis was conducted using Stoke's settling rate law via pipette analysis to separate the silt ($4 < x < 8\ \Phi$) and clay ($< 8\ \Phi$) particles once the sand ($> 4\ \Phi$) had been wet sieved out of the sample using a 64-micron mesh. The bulk densities were determined by using a laboratory scale to measure the mass of a known volume of sediment. Three to five replicates were performed for each sample to determine an average and for statistical analysis of the bulk density measurements. Water content, organic content, porosity, the solids fraction, and the sand fraction were also determined.

A portable veterinary x-ray source was used to project images of the sediment cores onto a digital x-ray panel. A lead-lined box was used to shield the x-rays produced as the sediment core was x-rayed. A PaxScan 4030A Amorphous Silicon Digital X-Ray Detector was used to digitize the images of the cores, and then Varian Image Viewing and Acquisition (VIVA) software was used to create 16-bit .tiff core images. The digital panel is sensitive to 2^16 (65,536) grey levels, which allows for excellent and accurate analysis of sediment cores. The panel has a theoretical resolution of 194 microns, allowing analysis of the sediment to be conducted on a sub-millimeter scale.

The x-ray generator was used with settings of 60 KVP for a time of 0.18 to 0.5 seconds per shot. Similar time settings are optimal to ensure the x-ray intensity is uniform between images. The cores from the first three sites were imaged with identical settings, but due to damage and subsequent repair of the x-ray source, there was a change in x-ray generation. The time setting was changed for the fourth site to determine optimal settings for imaging, and a time setting of 0.18 seconds was used for all the images from the fourth site.

An acrylic standard was created to use as a standard between x-ray images. The standard was not included in the x-ray images of the first three sites. It was included in the images from the fourth site so they could be intercalibrated to one another using the grayscale pixel values of the standard. The pixel values of each image were then calibrated to the average pixel value of the standard. This was to ensure that the grayscale values of the images corresponded to one another.

The MATLAB software environment was used to analyze the sediment data gathered and develop the plots and calibrations. The digital x-ray images were analyzed using MATLAB image analysis software to intercalibrate the images and to allow comparison to the laboratory measurements to be made.

Results:

Grayscale pixel values obtained using the digital flat panel were averaged across the core over the same depth intervals as the sediment analyses were performed. A comparison of the measured bulk densities and the averaged grayscale values was created in Figures 2 and 3 by plotting the grayscale values for all the sites against the measured bulk densities. Linear regression lines were fit to all of the data so calibrations could be developed. An exponential best fit line was also applied to the data to determine which was a better fit, but it was decided that linear regression was preferable to an exponential polynomial regression because it had a better fit to the data and correlated the values more closely. It is seen in Figure 2 that the individual sites have a higher slope than the slope for all the sites together. This is because the individual sites are shifted along the axes. These relationships were then used as calibrations to convert the x-ray grayscale values to bulk density.

Calibrations were also acquired for each individual site by using the same method as was done for all the sites together. The grayscale values were plotted against the measured bulk density values and linear regression fits lines were fitted to each data set. It is shown in Figure 3 that the R^2 values of the linear regression fits are much higher than the values of the fit to all the sites combined. It is also shown that the linear regression lines have a much better fit for the Goodwin Islands, VIMS Buoy, and Clay Banks Secondary Channel than for the fit for all the data combined. This holds true for all sites except the Clay Bank Main Channel, which has an R^2 value lower than the value for all

the sites combined. This is because the range of data in this site was extremely low, so small variations in the data resulted in a worse linear regression fit.

After developing the calibrations from the linear regression fit lines, we were able to apply these to the grayscale values obtained from the sediment cores and determine bulk density values of the sediment via the calibrations developed. Figures 5 and 6 show the values for measured bulk density, bulk density determined from the calibration using all the sites' data, and bulk density determined using the calibration from each individual site along core depth. As seen in Figure 5, the bulk density values for the Clay Banks Main Channel show that most of the values obtained using the calibration developed for the Clay Banks Main Channel fall within the standard error of the laboratory measured bulk densities. This is a very good calibration because the standard errors are extremely small. The calibration developed using all the sites data is also a pretty accurate calibration, but not as accurate as the calibration for the individual site.

Figure 4 shows the comparison of the measured bulk densities and the calibrated bulk densities using both calibrations for all of the individual sites. The general trend is that the bulk densities calculated from the individual site calibrations are closer to the measured values than the bulk densities calculated from the calibration acquired from all the sites combined. It is also seen that both calibrations produce accurate results, usually falling within about 0.05 g cm^{-3}. One can infer that using even the coarsest approach can still yield fairly decent results.

Discussion:

The comparisons of bulk density and grayscale values for the sites yielded a large range of calibrations developed from the linear regression lines. This result could be expected from varying sand and organic contents between the sites. Another possible explanation is that the variations in x-ray intensity and digital x-ray panel response could result in the grayscale pixel values not corresponding to each other for each site, as a standard was not included in the first three sites.

In nature, grain sizes should have a detectable effect on the attenuation of x-rays. This is because the composition of grains is different over the size classes. Sands are composed mostly of SiO_2, and silts and clays contain iron, aluminum, silicates, and other elements. The elemental composition will produce different linear attenuation coefficients between sand, silt, and clay, and this should have an effect upon the attenuation of the x-rays.

Although sand and organic content must have an effect upon the attenuation of x-rays, the effect was not discernable. By comparing the calibration slopes of the Clay Banks Main Channel to the organic and sand content, it was determined there was no apparent effect upon attenuation. The Clay Banks sites had the lowest slopes of the linear regression fits and the greatest variations in sand and organic content of the sites, as shown in Figure 6. One would expect that if there is an effect on x-ray attenuation by the sand and organic content, then the slopes of the Clay Banks sites would be at the extremes, but it does not have that affect.

Variation of sand and organic content between sites was not enough to be shown to have an effect through simple laboratory analysis. This shows that the effect upon attenuation of the sand and organic contents was small enough to be masked by the variations of the bulk density, which is the controlling factor in x-ray attenuation. While no obvious trends of the effect on attenuation by sand and organic contents were seen, more sites need to be sampled to obtain a larger range of sand and organic contents to be able to create a statistical analysis of the effect on x-ray attenuation of these factors.

The presence and amount of dissolved salts in sediment tends to have a very small affect on the attenuation of x-ray s (Coppola 1974), and since the changes in the amount of dissolved salts between the sites was very small (a change in about 10 ppt resulting in a change of about 0.006 g/ml in the density of water), the change in the mass attenuation coefficient of water was small enough to be negligible.

It is believed that by using the revised techniques as applied to samples from the Clay Banks Main Channel site in future analyses we will achieve a better correlation between bulk density and grayscale and we will find better agreement between sites. It is essential to conduct sediment analyses on the same sediment that is digitally imaged, and to include the same standard in all images to they can be intercalibrated to each other. If this was done then the calibrations acquired should have less variation, and the calibration acquired from all the sites combined should be much closer to the individual site calibrations. Since the individual sites did not have vastly different grain size and organic contents, they should have closer calibrations than that which was determined.

Applications:

There are many useful applications of this technique that relate to bulk density. It is possible to convert the grayscale pixel values obtained by the digital x-radiography panel into bulk density values, using the calibrations that were developed. This is useful because it creates a map of bulk density values on the sediment x-ray images, so one can look and see the changes of bulk density throughout the core. It is also possible to apply a false-color map to the image of bulk density values to bring out features and allow for better and easier interpretation. An example of this is shown in Figure 7, which is a false color image of sediment from the Clay Banks Main Channel. It is seen that the color map image brings out prominent features to a greater degree and makes the subtle features easier to distinguish. A low bulk density layer is found at the surface, possibly indicating an active layer with recent deposition, erosion, or resuspension. Laminated sediment is seen in the lower core and a burrow that has been filled in with lower bulk density sediment is seen along the left edge of the core. The color map allows simple identification of biological structures and other bioturbation processes. Digital x-radiography is a valuable tool for detailed core description and the verification of bioturbation and other biological structures (Lofi 2001). These are seen as low bulk density burrows and mixing of laminated sediment, seen in Figure 6 along the right edge of the burrow.

Another application of this calibration process is to create a bulk density profile and overlay it upon a sediment x-ray core, creating a profile much like the one developed by Wheatcroft (Wheatcroft 2005). This is shown in Figure 8 where a bulk density profile is superimposed on a digital x-ray sediment image containing the grayscale values. The grayscale values across the core image are averaged over a chosen depth interval, and then applied to the calibrations obtained to output a profile of bulk density over the depths chosen. Each pixel row (a depth interval of 194 microns) was averaged across the

core to look at small-scale variations in the core. The advantage of this application is that the bulk density overlay can be extended past the area sampled in laboratory measurements and bulk density values can be extrapolated by looking at the overlay. Another feature of this application is that if the chosen depth interval is very small one can view dramatic increases and decreases in bulk density over short ranges, as seen in Figure 8 at the surface layer.

Conclusion:

The development of this technique yielded useful results on many levels that relate to bulk density and the process of digital x-radiograph imaging. It was found that the pixel grayscale values generated by the digital x-ray panel are well correlated to the bulk density of the sediment. The correlation between the grayscale values and the bulk density measurements resulted in a very strong linear fit, making the development of a calibration equation very simple. The organic content and grain size fractions were found to have no obvious affect upon the attenuation of the x-ray. This may have been because the organic contents did not differ greatly site-to-site, making statistical analyses of the effect upon attenuation difficult due to the low range. Sand content did have a large range between the sites, but no apparent effect upon x-ray attenuation could be found due to the sand fraction.

We were able to convert the grayscale pixel values of the x-ray images into bulk density values using the calibrations developed. It was determined that the calibrations acquired from each individual site were more accurate than the calibrations acquired from all the sites combined. It is possible to develop a calibration that could be used for the entire York River if enough data were gathered. It is thought that a calibration for the entire river is possible and could work fairly well.

It was found that the calibrations developed could be used to extrapolate bulk density values between the depths measured and also beyond depths that were analyzed in laboratory experiments. This is extremely useful because it aids in sediment interpretation beyond laboratory measurements. The development of this technique can be further refined to achieve very high image resolution and provide insight into bed erosion and consolidation processes.

Acknowledgements:

Many Thanks are given to the guidance and overview of Patrick Dickhudt and Dr. Carl Friedrichs. Generous guidance on the usage of the digital x-radiograph was given by Dr. Steve Kuehl, Linda Menegheni, and Lila Gerald. Thanks are also given to Grace Cartwright and Heidi Romine for instruction on lab work. Drs. Rochelle Seitz and Jill Peloquin were influential in the development and editing of papers and programs, and in directing the Summer Intern Program. Funding was provided by the NSF for the Summer Intern Program at the Virginia Institute of Marine Science and by the VIMS Coastal Hydrodynamics and Sediment Dynamics Lab.

References:

Aylmore L.A.G. (1993) Use of Computer-Assisted Tomography in Studying Water Movement around Plant Roots. Advances in Agronomy, Vol. 49

Coppola M, Reiniger P. (1974) Influence of the Chemical Composition on the Gamma-Ray Attenuation by Soils. Soil Sciences, Vol. 117, No. 6: 331-335

Friedrichs CT, Diaz RJ, Harris CK, Kuehl SA, Schaffner LC (2005) Collaborative research: A real-time and rapid response observing system for the study of physical and biological controls on muddy seabed deposition, reworking and resuspension. Proposal to the National Science Foundation

Lofi J, Weber O (2001) SCOPIX – digital processing of X-ray images for the enhancement of sedimentary structures in undisturbed core slabs. Geo-Marine Letters 20: 182-186

Migeon S, Weber O, Faugeres J-C, Saint-Paul J (1999) SCOPIX: a new X-ray imaging system for core analysis. Geo-Marine Letters 18: 251-255

Orsi TH, Anderson AL (1999) Bulk density calibration for X-ray tomographic analyses of marine sediments. Geo-Marine Letters 19:270-274

Wheatcroft RA, Stevens AW, Hunt LM, Lewis RC (2005) The large-scale distribution and internal geometry of the Fall 2000 Po River flood deposit: evidence from digital x-radiography. Submitted to Continental Shelf Research

Figures:

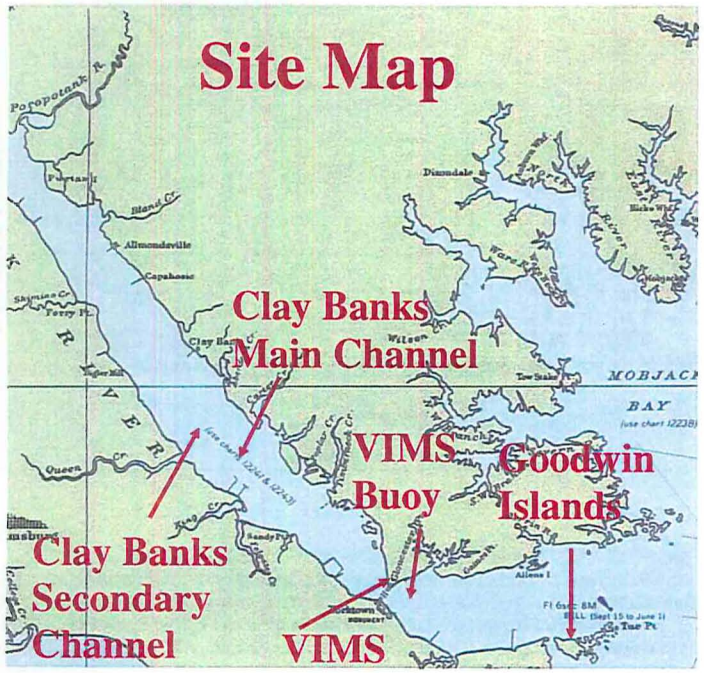

Figure 1:
Map of the lower York River, Virginia and arrows pointing to site sampling locations in reference to VIMS.

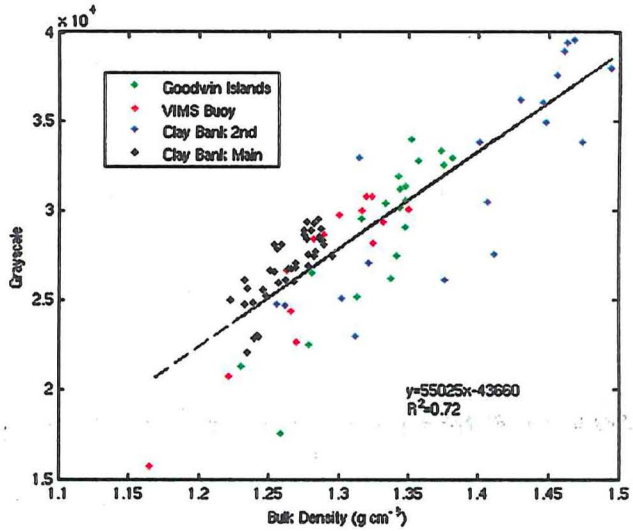

Figure 2:
Plot comparing measured bulk densities for all sites to the averaged grayscale values of the x-ray images. A linear regression fit was created and the R^2 value for the fit and the equation of the regression are included in the plot. The calibration for all sites was developed from this equation.

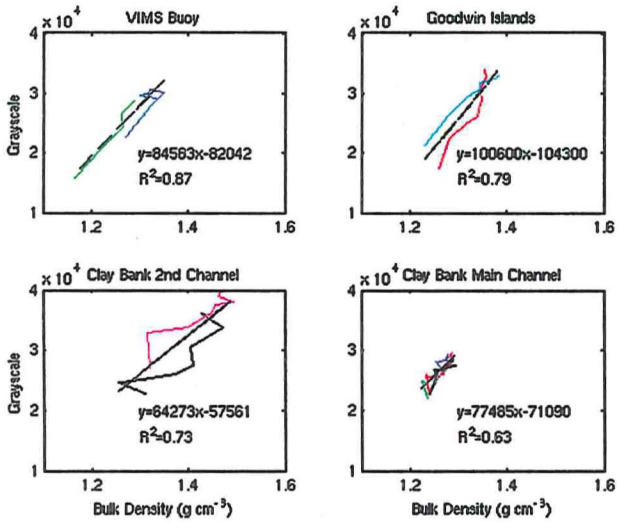

Figure 3:
Plot comparing the measured bulk density values for each site to the grayscale values each site. The individual R^2 values and the equations of the linear regression lines are included. The calibrations for each individual site are created using the linear regression equations.

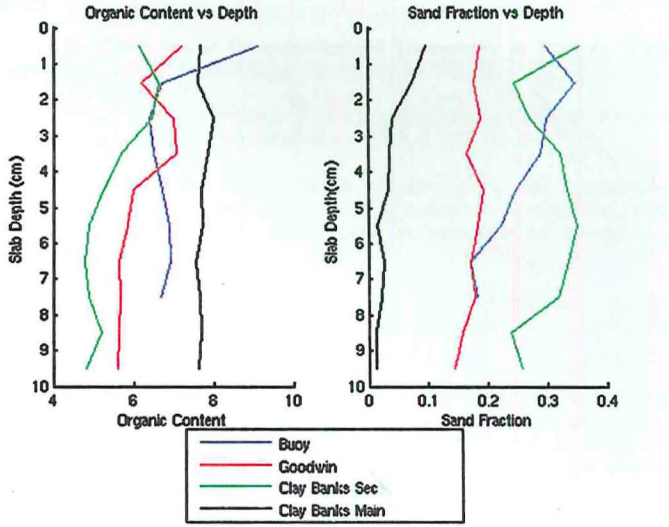

Figure 4:
Plots showing organic content and sand fraction along the depth of the cores from each site.

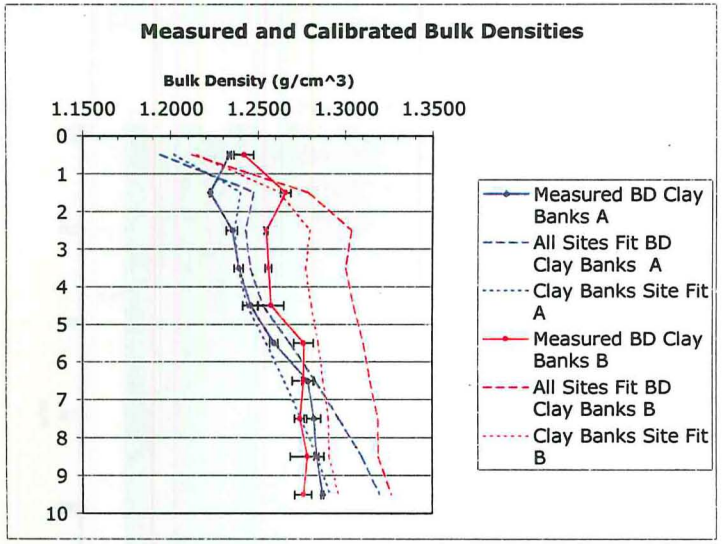

Figure 5:

Plot showing the measured bulk densities (solid line), bulk densities developed using the calibration equation from all sites combined (dashed line), and bulk densities developed using the calibration equation from the individual sites (dotted line) along the depth of the core. The standard error associated with the measured bulk densities is included for the sites. The sites shown are two cores from the Clay Banks Main Channel.

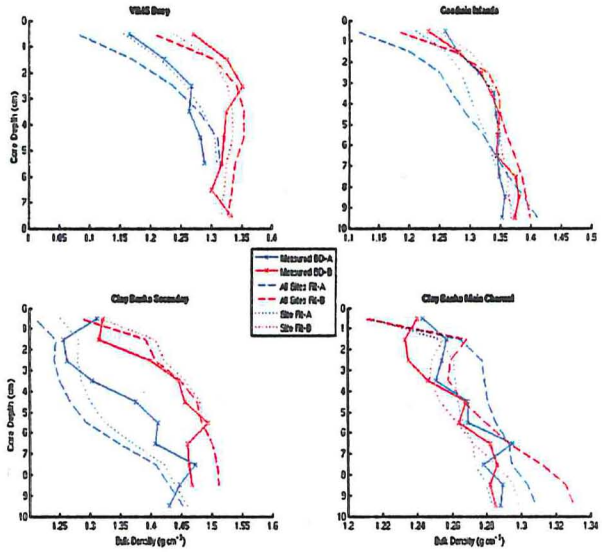

Figure 6:

Plot showing the measured bulk densities (solid line), bulk densities developed using the calibration equation from all sites combined (dashed line), and bulk densities developed using the calibration equation from the individual sites (dotted line) along the depth of the core for individual sites. The different colors correspond to different core samples from the same site.

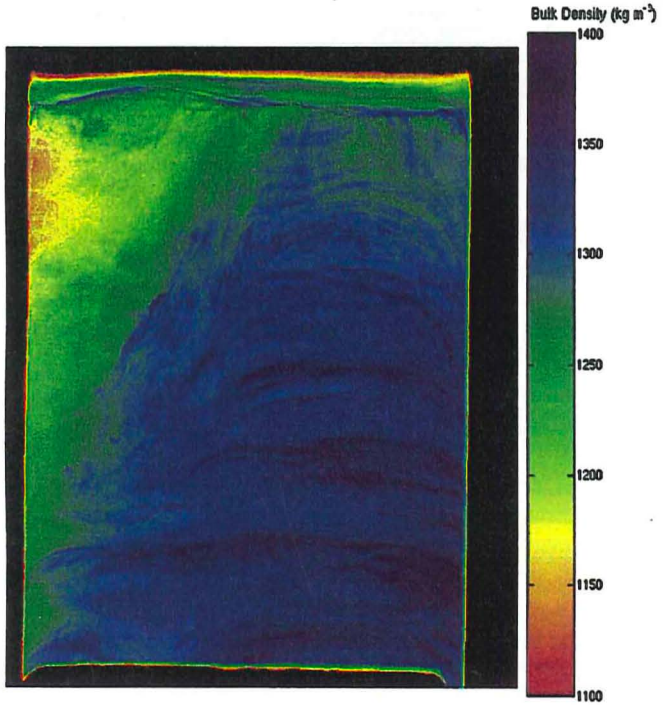

Figure 7:
False color map image of a core from the Clay Banks Main Channel. The grayscale values were converted to bulk density values using the site calibration and then a color map was applied to these values to bring out features of the core. The color scale corresponds to bulk density.

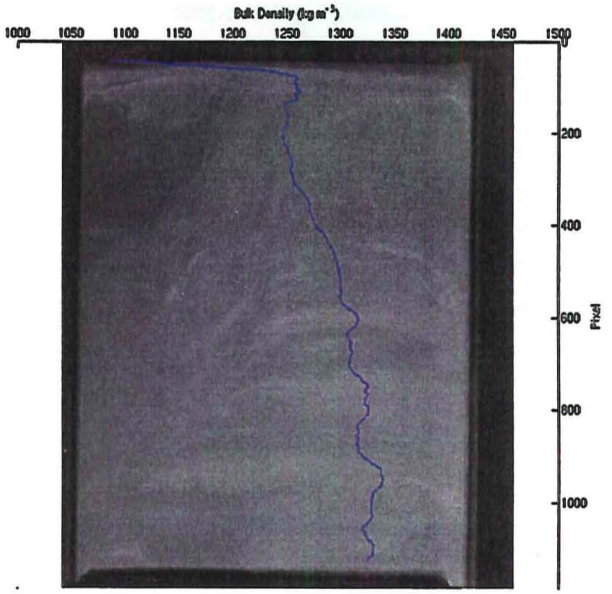

Figure 8:
Image of same core in Figure 6 showing averaged bulk density values with depth. The pixel values across the core were averaged for each pixel depth, and the calibration was used to determine the bulk density. Each pixel depth was 194 microns, and about 50 pixels correspond to a centimeter in depth along the y-axis. This image shows bulk density values can be extrapolated further than laboratory measurements, as laboratory measurements were conducted to a depth of 10 cm, around 500 pixels in this image.